A closed-form analytic solution for the P_L - S_N equations of neutron transport in slab geometry

1996 J. Phys. A: Math. Gen. 29 7137

(http://iopscience.iop.org/0305-4470/29/22/014)

J. Phys. A: Math. Gen. **29** (1996) 7137–7155. Printed in the UK

A closed-form analytic solution for the P_L–S_N equations of neutron transport in slab geometry

Charles H Aboughantous

Louisiana State University, Department of Physics and Astronomy, Baton Rouge, Louisiana 70803, USA

Received 9 April 1996, in final form 26 June 1996

Abstract. A closed-form analytic solution for the discrete-ordinates equations of neutron transport is obtained without recourse to integral transforms. The method is applied to the slab-geometry problem in the one-speed approximation using a one-sided set of boundary conditions. The solution is valid for any number of discrete ordinates and all possible orders of anisotropic scattering, and it does not require *a priori* knowledge of the particular solution. A set of algebraic expressions for the neutron balance at the boundaries of a slab is obtained and used as a basis for one iterative and one non-iterative numerical algorithm that are valid for all homogeneous and heterogeneous slabs. The numerical solutions are error free other than the roundoff of the computing system. The roundoff error is minimized by the Effective Albedo and Transmittance method.

1. Introduction

In the past few decades, a great amount of effort has been devoted to the development of methods that minimize the errors in neutron-transport computations using the discrete-ordinates method. In this endeavour, very few attempts were made using exact analytical methods. The original development of the discrete-ordinates method for radiative transfer by Chandrasekhar [1] was reproduced by Davison [2] with a fair amount of detail relevant to the neutron-transport problem. More recently, attempts were made, using the analytical method, to obtain exact expressions particularly useful for numerical applications in neutron transport in slab geometry [3, 4]; the method was subsequently implemented in the two-dimensional problem in plane geometry [5]. Other attempts exploited the integral transform method [6, 7].

The method outlined by Davison consists of a finite series of exponentials that satisfy the one-dimensional discrete-ordinates equation in plane geometry. The terms of the series are defined with two sets of parameters: a set of terms for the exponential argument and a set of coefficients. The terms of the first set are the zeros of a polynomial and the coefficients are to be determined from the boundary conditions. The half-space medium-boundary conditions and the vacuum-boundary condition were discussed. A marginal discussion about the continuity of flux-boundary condition was provided with an incomplete account on the treatment of the fixed source [2].

A more recent analytical approach exploited the spectral method [4]. The solution to the discrete-ordinate equation is exact but inherently iterative. The major shortcoming of the method is, as pointed out by its authors, its inability to operate with more than eight discrete ordinates. On the other hand, the handling of the high-order anisotropic scattering

0305-4470/96/227137+19$19.50

was not addressed convincingly. As to the handling of the source term, the method requires *a priori* knowledge of a particular solution to the problem. Although the solution is carried out in slab geometry, it was successfully implemented in the Cartesian two-dimensional geometry [5].

In another recent approach the Laplace transform was used to obtain analytic solutions to the one-dimensional plane-geometry problem. This method is applied to the P_1–S_N problem in the one-speed approximation [6] and P_0–S_N multigroup problem [7]. The method is valid in homogeneous and heterogeneous slabs and seems to be doing well for $N \leqslant 8$ in a near-pure scatterer medium and fairly well in a slightly absorptive but otherwise thin media.

In this paper the author pursues a direct approach to obtain a closed-form analytic solution for the general P_L–S_N problem of neutron transport in slab geometry and in the one-speed approximation. The solution obtained by this method accounts for anisotropic scattering up to $L = N - 1$.

The proposed closed-form solution was converted into algebraic expressions that are nothing but expressions for the neutron balance at the boundaries of the slab. Two numerical algorithms based on this form of the solution are proposed, the first one is iterative and the second is non-iterative, and both of the algorithms are valid for all homogeneous and heterogeneous slabs. The performance of this method is excellent even in absorbing and thick media.

2. Reduction of the discrete-ordinates equations

2.1. Matrix representation of the governing equation

The general form of the one group P_L–S_N discrete-ordinates transport equation with no fission in slab geometry may be written in the form

$$\mu_m \partial_x \Psi_m + \sigma_t \Psi_m = \sum_{n=1}^{N} \left\{ \sum_{l=0}^{L} \frac{2l+1}{2} \sigma_l w_n P_l(\mu_m) P_l(\mu_n) \right\} \Psi_n + q_m \qquad (2.1)$$

where ∂_x is the symbol of derivative with respect to x, and

$\Psi_m \equiv \Psi(x, \mu_m); \qquad m = 1, 2, \ldots, N$ (N even)

$\mu_m =$ directional cosine on $(-1, 1) - \{0\}$

$w_n =$ weight for Gauss–Legendre quadrature

$P_l(\mu_m) =$ Legendre polynomial, $l = 0, 1, 2, \ldots, L \leqslant N - 1$

$\sigma_t =$ macroscopic total cross section

$\sigma_l = l$th scattering moments

$q_m \equiv q(x, \mu_m)$, a fixed source.

The domain of definition of (2.1) is a homogeneous slab of thickness h, bounded by the 0-boundary at $x = 0$ and by the h-boundary at $x = h$. We will assume that (2.1) is defined on a consistent set of cross sections:

$$\{\sigma_t, \sigma_l\} \equiv \{\sigma_t, \sigma_l; l = 0, 1, \ldots, N-1 \mid \sigma_t \geqslant \sigma_0 > |\sigma_1| > \cdots > |\sigma_{N-1}| > 0\}. \qquad (2.2)$$

Condition (2.2) prevails throughout the analysis.

Equations (2.1) are a set of N coupled equations subject to boundary conditions we will introduce later. We split this set into two subsets of N' coupled equations, one for

the backward direction and the other for the forward direction. Superscript minus and plus signs will be used to designate backward and forward properties, respectively, as follows:

$$\begin{aligned} &\text{Forward direction: } \mu_m^+ \equiv \mu_m > 0 \qquad \Psi_m^+ \equiv \Psi(x, \mu_m^+) \\ &\text{Backward direction: } \mu_m^- \equiv -\mu_m \qquad \Psi_m^- \equiv \Psi(x, \mu_m^-) \end{aligned}$$

where $m \in [1, N']$, $\mu_{N'} > \cdots > \mu_2 > \mu_1 > 0$, $N' = N/2$. These notations will be used throughout and the characterization forward and backward properties should always be understood in the context of these definitions.

The following two sets of backward and forward equations can be obtained from (2.1):

$$\begin{aligned} \mu_m^- \partial_x \Psi_m^- + \sigma_t \Psi_m^- = \sum_{n=1}^{N'} \Bigg\{ \Bigg(\sum_{l=0}^{L} \frac{2l+1}{2} \sigma_l w_n P_l(\mu_m^-) P_l(\mu_n^-) \Bigg) \Psi_n^- \\ + \Bigg(\sum_{l=0}^{L} \frac{2l+1}{2} \sigma_l w_n P_l(\mu_m^-) P_l(\mu_n^+) \Bigg) \Psi_n^+ \Bigg\} + q_m^- \end{aligned} \tag{2.3}$$

$$\begin{aligned} \mu_m^+ \partial_x \Psi_m^+ + \sigma_t \Psi_m^+ = \sum_{n=1}^{N'} \Bigg\{ \Bigg(\sum_{l=0}^{L} \frac{2l+1}{2} \sigma_l w_n P_l(\mu_m^+) P_l(\mu_n^-) \Bigg) \Psi_n^- \\ + \Bigg(\sum_{l=0}^{L} \frac{2l+1}{2} \sigma_l w_n P_l(\mu_m^+) P_l(\mu_n^+) \Bigg) \Psi_n^+ \Bigg\} + q_m^+. \end{aligned} \tag{2.4}$$

Owing to the symmetry properties of Legendre polynomials the following parameters may be defined:

$$c_l = \sigma_l / \sigma_t < 1$$

$$W_{ln} = (2l+1) c_l w_n \tag{2.5a}$$

$$W_{ln} P_l(\mu_m^+) P_l(\mu_n^+) = W_{ln} P_l(\mu_m^-) P_l(\mu_n^-) = G_{lmn} \in (-1, +1) \tag{2.5b}$$

$$W_{ln} P_l(\mu_m^+) P_l(\mu_n^-) = W_{ln} P_l(\mu_m^+) P_l(\mu_n^+) = (-1)^l G_{lmn} \tag{2.5c}$$

$$m, n \in [1, N'].$$

The G_{lmn} parameters enjoy the following properties:

$$\left.\begin{aligned} &\text{Pure absorber: } G_{lmn} = 0 \qquad \forall l, m, n > 0 \\ &\text{Isotropic scattering: } G_{0mn} = W_{0n} \qquad \forall m, n > 0 \end{aligned}\right\}. \tag{2.6}$$

Multiply (2.3) by $-h/\mu_m$ and (2.4) by h/μ_m and rearrange to obtain

$$\partial_\zeta \Psi_m^- = \frac{\beta_{tm}}{2} \sum_{n=1}^{N'} \Bigg\{ \Bigg(2\delta_{mn} - \sum_{l=0}^{L} G_{lmn} \Bigg) \Psi_n^- - \Bigg(\sum_{l=0}^{L} (-1)^l G_{lmn} \Bigg) \Psi_n^+ \Bigg\} - Q_m^- \tag{2.7}$$

$$\partial_\zeta \Psi_m^+ = \frac{\beta_{tm}}{2} \sum_{n=1}^{N'} \Bigg\{ -\Bigg(2\delta_{mn} - \sum_{l=0}^{L} G_{lmn} \Bigg) \Psi_n^+ + \Bigg(\sum_{l=0}^{L} (-1)^l G_{lmn} \Bigg) \Psi_n^- \Bigg\} + Q_m^+ \tag{2.8}$$

where

$$\beta_{tm} \equiv \frac{h \sigma_t}{\mu_m} \qquad m = 1, 2, \ldots, N' \tag{2.9}$$

$$Q_m^\pm \equiv \frac{h}{\mu_m} q_m^\pm(\zeta) \tag{2.10}$$

$\zeta = \dfrac{x}{h} \in [0, 1]$, the new dimensionless independent variable

δ_{mn} = Kronecker delta.

In ζ coordinates, the slab is defined by its 0-boundary at $\zeta = 0$ and h-boundary at $\zeta = 1$.

Define the dimensionless parameters:

$$a_{mn} \equiv \frac{\beta_{tm}}{2}\left[2\delta_{mn} - \sum_{l=0}^{L} G_{lmn}\right] \tag{2.11}$$

$$a^*_{mn} = \frac{\beta_{tm}}{2}\sum_{l=0}^{L}(-1)^l G_{lmn}. \tag{2.12}$$

It can be shown that, if

$$\omega^o_{mn} = \frac{\beta_{tm}}{2}\left(\delta_{mn} - \sum_{l=1}^{L} G_{lmn}\right)_{\text{odd } l} \tag{2.13}$$

and

$$\omega^e_{mn} = \frac{\beta_{tm}}{2}\left(\delta_{mn} - \sum_{l=0}^{L-1} G_{lmn}\right)_{\text{even } l} \tag{2.14}$$

then

$$\left.\begin{aligned} a_{mn} &= \omega^o_{mn} + \omega^e_{mn} \\ a^*_{mn} &= \omega^o_{mn} - \omega^e_{mn} \end{aligned}\right\} \tag{2.15}$$

and

$$|a_{mm}| > |a_{mn}| > |a^*_{mn}| \geqslant 0 \qquad \forall m, n. \tag{2.16}$$

Rewrite (2.7) and (2.8) in terms of identities (2.11) and (2.12):

$$\partial_\zeta \Psi^-_m = \sum_{n=1}^{N'} a_{mn}\Psi^-_n - \sum_{n=1}^{N'} a^*_{mn}\Psi^+_n - Q^-_m \tag{2.17}$$

$$\partial_\zeta \Psi^+_m = \sum_{n=1}^{N'} a^*_{mn}\Psi^-_n - \sum_{n=1}^{N'} a_{mn}\Psi^+_n + Q^+_m. \tag{2.18}$$

Define the submatrices:

$$\left.\begin{aligned} A &= [a_{mn}] \qquad & A^* &= [a^*_{mn}] \\ \Psi^\pm &= \{\Psi^\pm_m\} \qquad & Q^\pm &= \{Q^\pm_m\} \end{aligned}\right\}. \tag{2.19}$$

In (2.19), A and A^* are dimensionless constant-coefficient square matrices and $\Psi^\pm$ and $Q^\pm$ are column vector-valued functions of ζ. Two particular cases are worth noting: for a pure absorber, A is a diagonal and A^* is a null matrix, and, with isotropic scattering $a_{mn} = -a^*_{mn}$ for $m \neq n$, and $a_{mm} > a^*_{mm} > 0$. Note that the notation A^* is not intended to mean the conjugate matrix of A and that should not introduce any confusion.

Equations (2.17) and (2.18) can be merged into one P_L–S_N matrix equation:

$$\partial_\zeta \begin{Bmatrix} \Psi^- \\ \Psi^+ \end{Bmatrix} = \begin{bmatrix} A & -A^* \\ A^* & -A \end{bmatrix} \begin{Bmatrix} \Psi^- \\ \Psi^+ \end{Bmatrix} + \begin{Bmatrix} -Q^- \\ Q^+ \end{Bmatrix}. \tag{2.20}$$

Further formal simplification of (2.20) may be obtained by defining the matrices:

$$\Psi = \Psi^- \cup \Psi^+ \equiv \begin{Bmatrix} \Psi^- \\ \Psi^+ \end{Bmatrix} \qquad \boldsymbol{Q} \equiv \begin{Bmatrix} -Q^- \\ Q^+ \end{Bmatrix} \qquad \Lambda \equiv \begin{bmatrix} A & -A^* \\ A^* & -A \end{bmatrix}. \tag{2.21}$$

Then the reduced P_L–S_N matrix equation becomes

$$\partial_\zeta \Psi = \Lambda\Psi + \boldsymbol{Q}. \tag{2.22}$$

Vectors Ψ and $\boldsymbol{Q}$ of (2.22) are valued functions in ζ, and Λ is a dimensionless constant coefficient matrix. Notice that, by inequalities (2.16), Λ is diagonally dominant and none of its diagonal terms are zero.

2.2. The boundary conditions

The conventional practice in discrete-ordinates formalism is to impose on (2.1), or equivalently on (2.22), a natural boundary condition of entering fluxes at both edges of the slab [8]. In the present analysis we will deviate from this practice and impose one-sided boundary conditions at $\zeta = 0$:

$$\left.\begin{array}{l}\text{entering flux: } \Psi_0^+ \equiv \Psi^+(\zeta = 0)\\ \text{exiting flux: } \Psi_0^- \equiv \Psi^-(\zeta = 0)\end{array}\right\} \Leftrightarrow \Psi_0 \equiv \Psi(\zeta = 0). \tag{2.23}$$

We recognize that this set of boundary conditions is not natural: entering and exiting fluxes at the same boundary are assumed known *a priori*. This is an admittedly unrealistic assumption since Ψ_0^- becomes available only after the solution is reached, but it is harmless. This boundary condition is merely a matter of convenience intended to initiate the solution for equation (2.22) over its domain of definition. The apparent inconsistency that the solution, Ψ_0^-, is itself a boundary condition is merely an introductory step in the solution. We are by no means relieved from the constraint of entering flux-boundary condition Ψ_h^- at the right edge of the slab, the h-boundary, or eventually a vacuum-boundary condition $\Psi_h^- = \mathbf{0}$. The natural boundary conditions will be restored later in the solution.

The one-sided boundary condition was previously implemented in the solution of the discrete-ordinates problem of neutron transport [6, 7]. The Laplace transform method was used to solve the equations and that necessitated the use of this type of boundary condition. In the present work we imposed this boundary condition on the problem intentionally and it is not peculiar to the method of solution. It is formulated in this paper as a mathematical tool with the expectation that it can be exploited in other types of problems governed by second-order differential equation as well.

3. The closed-form solution

With the prescribed one-sided boundary conditions configurations (2.23), the formal solution for (2.22) is trivial:

$$\Psi = \mathrm{e}^{\zeta\Lambda}\Psi_0 + \int_0^1 \mathrm{e}^{(\zeta - s)\Lambda}\boldsymbol{Q}(s)\,\mathrm{d}s \tag{3.1}$$

where the matrix exponential can be expressed in terms of the eigenvalues of matrix Λ. It will be assumed throughout that vector $\boldsymbol{Q}$ is such that the integral of (3.1) can be obtained in closed form.

3.1. Properties of matrix Λ

The extraction of a physically meaningful solution from (3.1) depends largely on the existence and the nature of the eigenvalues of Λ. Useful properties of matrix Λ are summarized by the following theorems.

Theorem 1. For any set $\{\sigma_t, \sigma_l\}$ defined by (2.2), and for any even N, matrix Λ has N' distinct pairs of real opposite eigenvalues:

$$\lambda_1 > \lambda_2 > \cdots > \lambda_{N'} > 0 > -\lambda_{N'} > \cdots > -\lambda_2 > -\lambda_1.$$

Theorem 2. For n positive integer, the nth power of Λ is a matrix of the form

$$\Lambda^n = \begin{bmatrix} X_n & (-1)^n Y_n \\ Y_n & (-1)^n X_n \end{bmatrix}$$

where X_n and Y_n are $N' \times N'$ square matrices corresponding to the nth power of matrix Λ.

Corollary 1. The diagonal elements of submatrix Y_n are all 0, $\forall n$ even.

The proofs of these theorems by recursion are straightforward.

From theorem 2 we have

$$X_1 = A \qquad Y_1 = A^*$$
$$X_n = X_{n-1}A + (-1)^{n-1} Y_{n-1} A^* \qquad n \geqslant 2$$
$$Y_n = Y_{n-1}A + (-1)^{n-1} X_{n-1} A^* \qquad n \geqslant 2$$

and

$$\operatorname{tr} \Lambda^n = 0 \qquad n \text{ odd}$$
$$\operatorname{tr} \Lambda^n = 2 \operatorname{tr} X_n \qquad n \text{ even.}$$

3.2. The explicit statement of the solution

Let $\boldsymbol{V}^k$ be the eigenvector corresponding to the kth eigenvalue λ_k, then the fundamental matrix $F(\zeta)$ of (2.22) is defined as follows:

$$F(\zeta) = [\boldsymbol{V}^1 \mathrm{e}^{\lambda_1 \zeta}\, \boldsymbol{V}^2 \mathrm{e}^{\lambda_2 \zeta}\, \ldots][\boldsymbol{V}^1\, \boldsymbol{V}^2\, \ldots]^{-1} \tag{3.2}$$

where all λ_k are real. Then (3.1) becomes

$$\Psi(\zeta) = F(\zeta)\Psi_0 + \int_0^\zeta F(\zeta - s)\boldsymbol{Q}(s)\, \mathrm{d}s. \tag{3.3}$$

By our choice of vector $\boldsymbol{Q}$, the integral in the right side of (3.3) can be evaluated in closed form. In what follows, the source is assumed isotropic and uniformly distributed, but the procedure of extracting the explicit solution from (3.3) is applicable to the general case of a non-uniformly distributed source.

With $\boldsymbol{Q}$ a constant vector, the integration of matrix $F(\zeta - s)$ is elementary. Define the square matrix

$$G(\zeta) = \int_0^\zeta F(\zeta - s)\, \mathrm{d}s. \tag{3.4}$$

Then (3.3) takes the form

$$\Psi = F(\zeta)\Psi_0 + G(\zeta)\boldsymbol{Q}. \tag{3.5}$$

Equation (3.5) is the general solution for (2.1) for the prescribed one-sided boundary condition (2.23) represented by the vector $\Psi_0 = \Psi_0^- \cup \Psi_0^+$ defined by (2.21). However, this solution is incomplete. The exiting-flux vector Ψ_0^- is yet to be determined. To complete the solution, we seek an auxiliary equation from the solution itself. Partition the coefficient square matrices in (3.5) as follows:

$$F(\zeta) = \begin{bmatrix} \Phi_{11}(\zeta) & \Phi_{12}(\zeta) \\ \Phi_{21}(\zeta) & \Phi_{22}(\zeta) \end{bmatrix} \tag{3.6}$$

and

$$G(\zeta) = \begin{bmatrix} \Gamma_{11}(\zeta) & \Gamma_{12}(\zeta) \\ \Gamma_{21}(\zeta) & \Gamma_{22}(\zeta) \end{bmatrix} \tag{3.7}$$

where submatrices $\Phi_{mn}(\zeta)$ and $\Gamma_{mn}(\zeta)$ are $N' \times N'$ matrix valued functions of ζ. Then (3.5) may be reproduced as follows:

$$\begin{Bmatrix} \Psi^- \\ \Psi^+ \end{Bmatrix} = \begin{bmatrix} \Phi_{11}(\zeta) & \Phi_{12}(\zeta) \\ \Phi_{21}(\zeta) & \Phi_{22}(\zeta) \end{bmatrix} \begin{Bmatrix} \Psi_0^- \\ \Psi_0^+ \end{Bmatrix} + \begin{bmatrix} \Gamma_{11}(\zeta) & \Gamma_{12}(\zeta) \\ \Gamma_{21}(\zeta) & \Gamma_{22}(\zeta) \end{bmatrix} \begin{Bmatrix} -Q^- \\ Q^+ \end{Bmatrix}. \tag{3.8}$$

The first row in (3.8) may be evaluated at $\zeta = 1$ to obtain the following equation:

$$\Psi_h^- = \phi_{11}\Psi_0^- + \phi_{12}\Psi_0^+ - g_{11}Q^- + g_{12}Q^+ \tag{3.9}$$

where ϕ_{mn} and g_{mn} are dimensionless square matrices defined as follows:

$$\left.\begin{aligned} \phi_{mn} &\equiv \Phi_{mn}(\zeta = 1) \\ g_{mn} &\equiv \Gamma_{mn}(\zeta = 1) \end{aligned}\right\}. \tag{3.10}$$

It is apparent that (3.9) contains only one unknown, Ψ_0^-, the other flux vectors Ψ_0^+ and Ψ_h^- are the natural boundary conditions.

Considering that the fundamental matrix is constructed from eigenvectors of Λ, i.e. its columns are linearly independent, then matrix $F(\zeta)$ and its partition ϕ_{11} are not singular. Hence, the inverse matrix ϕ_{11}^{-1} exists and (3.9) can be solved for the unknown vector Ψ_0^-. Therefore, (3.8) and the auxiliary equation (3.9) are the complete closed-form solution of (2.1) with a uniformly distributed source, subject to the usual natural-boundary conditions of entering fluxes at both edges of the slab. This is the pointwise form of the solution.

4. The end-points solution

The key success of this method lies in the fact that matrix ϕ_{11} is invertible. Evaluate the second row in (3.8) at $\zeta = 1$ and substitute for Ψ_0^- from (3.9) to obtain the following expressions:

$$\Psi_0^- = \phi_{11}^{-1}\Psi_h^- + [-\phi_{11}^{-1}\phi_{12}]\Psi_0^+ + [\phi_{11}^{-1}g_{11}]Q^- - [\phi_{11}^{-1}g_{12}]Q^+ \tag{4.1}$$

$$\Psi_h^+ = [\phi_{21}\phi_{11}^{-1}]\Psi_h^- + [\phi_{22} - \phi_{21}\phi_{11}^{-1}\phi_{12}]\Psi_0^+ - [g_{21} - \phi_{21}\phi_{11}^{-1}g_{11}]Q^- + [g_{22} - \phi_{21}\phi_{11}^{-1}g_{12}]Q^+ \tag{4.2}$$

where all the coefficients are square matrices. Equations (4.1) and (4.2) are expressions for the exiting-flux vector at 0-boundary and h-boundary, respectively, as a concurrent contribution from all entering fluxes at both edges of the slab (the natural boundary conditions) and from the emission of source neutrons within the slab. Neither one of these two equations contains information about the distribution of neutrons within the slab. Hence, together (4.1) and (4.2) are the *end-points* solution for the transport equations (2.1).

4.1. The solution in radiation transport formalism

4.1.1. Radiative properties of a homogeneous slab. The coefficients in the right-hand sides of (4.1) and (4.2) are dimensionless square matrices. They are special operators that extract from the respective operands the appropriate contribution to the exiting flux at the specified boundary. The physical significance of these operators may be extracted from the nature of their operation on their operands. Of interest to our problem are the following properties.

(a) *Transmittance.* Without loss of generality, assume that the slab is sourceless, its h-boundary is exposed to a boundary flux $\Psi_h^- \neq \mathbf{0}$ and its 0-boundary is a free surface surrounded by a vacuum, i.e. $\Psi_0^+ = \mathbf{0}$. Let $\tau \equiv \phi_{11}^{-1}$. Then (4.1) reduces to

$$\Psi_0^- = \tau\Psi_h^- = \phi_{11}^{-1}\Psi_h^-. \tag{4.3}$$

Considering that ϕ_{11} is a diagonally dominant square matrix and is defined from properties of the slab, then τ itself is a property of the slab and all of its elements are dimensionless and less than unity. On the other hand, it is apparent that expression (4.3) is a transmission operation: on entering a backward flux vector Ψ_h^- at the h-boundary it is then transmitted through the slab as vector Ψ_0^- at 0-boundary. These properties adhere the significance of a *transmittance matrix* of the slab to τ. Using tensor notation, (4.3) takes the form

$$\Psi_{0m}^- = \tau_m^n \Psi_{hn}^- \qquad m, n = 1, 2, \ldots, N'. \tag{4.4}$$

In (4.4) and in all subsequent expressions the summation is implied on the repeated index. The significance of (4.4) is that each row component of τ projects the entering fluxes in all n directions at h-boundary into one exiting flux in the mth direction at 0-boundary.

In radiation theory, a scalar transmittance is defined as the ratio of the entering flux at one boundary to the exiting flux at the opposing boundary. In neutronics, this definition is expressed as the ratio of the exiting current, say J_0^-, to the entering current J_h^- at the opposite side of the slab:

$$\tau_s = \frac{J_0^-}{J_h^-} = \frac{\varpi^m \Psi_{0m}^-}{\varpi^m \Psi_{hm}^-} \tag{4.5}$$

where $\varpi^m = w_m \mu_m$. It is apparent from (4.5) that τ_s is a property of the slab distinct from τ_m^n: the former is a transformation in $\mathbb{R}$, the latter in $\mathbb{R}^{N' \times N'}$. For a pure absorber we will have

$$\Psi_{0m}^- = \tau_m^m \Psi_{hm}^- \Rightarrow \tau_m^m = \frac{\Psi_{0m}^-}{\Psi_{hm}^-} \neq \frac{J_0^-}{J_h^-} = \tau_s. \tag{4.6}$$

Only in the particular case of $N = 2$, does τ_m^n reduce to the scalar $\tau_1^1 = \tau_s$ for all slabs.

(b) *Albedo.* Without loss of generality, we assume that the slab is sourceless and without the entering flux at h-boundary. Then (4.1) reduces to

$$\Psi_0^- = \alpha \Psi_0^+ = [-\phi_{11}^{-1} \phi_{12}] \Psi_0^+. \tag{4.7}$$

The elements of matrix α defined by (4.7) are, like those of ϕ_{11}^{-1}, dimensionless, less than unity and are defined from physical and geometric properties of the slab. Therefore, matrix α is another property of the slab. It extracts the appropriate fractions from the entering-flux vector Ψ_0^+ at 0-boundary and projects them backwards as an exiting-flux vector Ψ_0^- at the same boundary; this is a reflection process. Considering that this reflection is 'volumetric', i.e. from the whole slab as opposed to specular at the surface of the slab, operator α takes the meaning of *albedo matrix* of the slab. Using tensor notation, (4.7) reads

$$\Psi_{0m}^- = \alpha_m^n \Psi_{0n}^+ \qquad m, n = 1, 2, \ldots, N'. \tag{4.8}$$

It is apparent from (4.8) that the mth row of matrix α transforms the entering fluxes in all n directions at 0-boundary into one exiting flux in the mth direction at the same boundary.

A scalar albedo is defined as the ratio of exiting current, say J_0^-, to the entering current, say J_0^+, at the same boundary:

$$\alpha_s = \frac{J_0^-}{J_0^+} = \frac{\varpi^m \Psi_{0m}^-}{\varpi^m \Psi_{0m}^+}. \tag{4.9}$$

Clearly, α_s and α_m^n are distinct: the former is a transformation in $\mathbb{R}$, the latter in $\mathbb{R}^{N' \times N'}$. Only in the particular case of $N = 2$, the albedo matrix reduces to the scalar $\alpha_1^1 = \alpha_s$. Note that in the case of a pure absorber, A^* of (2.19) and hence ϕ_{12} of (4.7) are null matrices with the result $\alpha = \mathbf{0}$ and $\alpha_s = 0$.

(c) *Radiance.* Consider a slab with a distributed source and its edges are surrounded by a vacuum. Assume further that no entrant-boundary fluxes are imposed on the slab, i.e. $\Psi_0^+ = \Psi_h^- = \mathbf{0}$. Then (4.1) reduces to

$$\Psi_0^- = \rho_0^- = \tau[g_{11}Q^- + (-g_{12})Q^+]. \tag{4.10}$$

Identity (4.10) expresses quantitatively the amount of source neutrons radiating outward in the backward direction at 0-boundary. Hence, we ascribe to ρ_0^- the significance of *radiance vector* of the slab at the prescribed boundary; the vectors embraced by square brackets in (4.10) are backward *emittance vectors* evaluated at h-boundary by the operation of g_{11} and g_{12} on the source vectors. Note, the simple explicit transformation of the source into emittance vectors as in (4.10) is peculiar to the present application of a uniformly distributed isotropic source. It is not expected to be that simple in the general case of arbitrarily distributed sources.

4.1.2. The neutron-balance statement of the solution. In light of the foregoing, (4.1) may be written as

$$\Psi_0^- = \tau\Psi_h^- + \alpha\Psi_0^+ + \rho_0^-. \tag{4.11}$$

An expression for the exiting flux at h-boundary formally similar to (4.11) can be obtained simply by recognizing that the transport process through a homogeneous slab is invariant under rotation of the slab about its axis of symmetry at the midplane. This is always true in the following cases: a sourceless slab, and an isotropic source symmetric about the midplane of the slab. It follows that by exchanging the roles of α and τ in (4.11) we obtain the expression for the exiting flux at h-boundary:

$$\Psi_h^+ = \alpha\Psi_h^- + \tau\Psi_0^+ + \rho_h^+. \tag{4.12}$$

Equation (4.12) can be obtained directly from (4.2) in the same way (4.11) is obtained from (4.1), with the results:

$$\tau = \phi_{11}^{-1} = \phi_{22} - \alpha\phi_{12} \tag{4.13}$$

$$\alpha = -\tau\phi_{12} = \phi_{21}\tau \tag{4.14}$$

$$\rho_0^- = \tau g_{11}Q^- - \tau g_{12}Q^+ \tag{4.15}$$

$$\rho_h^+ = (g_{22} - \alpha g_{12})Q^+ - (g_{21} - \alpha g_{11})Q^- \tag{4.16}$$

$$\rho_h^+ = \rho_0^-. \tag{4.17}$$

Identity (4.17) holds in the present application of a uniformly distributed isotropic source. It is also valid if the source is isotropic but otherwise symmetric about the midplane of the slab. In the general case of an arbitrarily distributed anisotropic source in a homogeneous slab, identity (4.17) is not valid and ρ_0^- and ρ_h^+ should be calculated separately.

Equations (4.11) and (4.12) are two uncoupled-expression solutions for the transport equation. They are indeed two quantitative expressions for the neutron balance at the boundaries of the slab, in the forward and the backward directions, and may be expressed verbally as follows:

$$\text{(exiting neutrons at a boundary)} = \begin{cases} \text{(neutrons transmitted through the slab)} \\ +\text{(reflected fraction of entering neutrons)} \\ +\text{(exiting neutrons that are produced within} \\ \text{the slab).} \end{cases}$$

Therefore, the Boltzmann equation, and its end-points solution, are merely two statements of the neutron balance in a slab. The former is a balance in differential formalism, the latter is algebraic.

4.2. Condensed and computational representation of the end-points solution

Equations (4.11) and (4.12) can be united into one matrix equation:

$$\begin{Bmatrix} \Psi_0^- \\ \Psi_h^+ \end{Bmatrix} = \begin{bmatrix} \tau & \alpha \\ \alpha & \tau \end{bmatrix} \begin{Bmatrix} \Psi_h^- \\ \Psi_0^+ \end{Bmatrix} + \begin{Bmatrix} \rho_0^- \\ \rho_h^+ \end{Bmatrix}. \tag{4.18}$$

Define the following matrices:

$$\text{Exiting-flux vector: } \Psi_{ex} = [\Psi_0^- \ \Psi_h^+]^T \tag{4.19}$$

$$\text{Entering-flux vector: } \Psi_{en} = [\Psi_h^- \ \Psi_0^+]^T \tag{4.20}$$

$$\text{Slab-radiance vector: } \boldsymbol{R} = [\rho_0^- \ \rho_h^+]^T \tag{4.21}$$

$$\text{Transport matrix: } \boldsymbol{T} = \begin{bmatrix} \tau & \alpha \\ \alpha & \tau \end{bmatrix}. \tag{4.22}$$

Then (4.18) reduces to the simple condensed form:

$$\Psi_{ex} = \boldsymbol{T}\Psi_{en} + \boldsymbol{R}. \tag{4.23}$$

For computational purposes, however, it is more convenient to write the solution using tensor notation as follows:

$$\left.\begin{aligned} \Psi_{0m}^- &= \tau_m^n \Psi_{hn}^- + \alpha_m^n \Psi_{0n}^+ + \rho_{0m}^- \\ \Psi_{hm}^+ &= \alpha_m^n \Psi_{hn}^- + \tau_m^n \Psi_{0n}^+ + \rho_{hm}^+ \end{aligned}\right\} \tag{4.24}$$

$$m, n = 1, 2, \ldots, N'.$$

In light of identity (4.17), the radiance terms of (4.24) are identically the same for each direction m. The superscript plus and minus signs are used merely for notational consistency.

5. An application to the end-points solution

Consider the case of a homogeneous sourceless slab and suppose that its 0-boundary is exposed to vector boundary flux Ψ_0^+ and its h-boundary surrounded with vacuum. Then:

$$\text{Leakage rate} = \{\varpi\}^T(\alpha + \tau)\Psi_0^+ \tag{5.1}$$

$$\text{Absorption rate} = \{\varpi\}^T(\boldsymbol{I} - \alpha - \tau)\Psi_0^+ \tag{5.2}$$

where $\boldsymbol{I}$ is the identity matrix. Equation (5.2) is, indeed, the rate of production of new atoms created within the slab. It can be used to calculate the rate of transmutations within the material without recourse to extensive and expensive flux calculations within the slab. Clearly, matrix $\Sigma = \boldsymbol{I} - \alpha - \tau$ of (5.2) represents a neutron sink property of a slab. If the slab is heterogeneous, α and τ of (5.1) and (5.2) should be replaced by their effective values defined below.

6. The stratified slab problem

The end-points solution expressed by (4.24) is exact and theoretically valid for an arbitrarily thick homogeneous slab. Unfortunately, finite arithmetics of digital systems imposes limitations on the thickness of the slab. Large optical thicknesses could invalidate the

answers by way of loss of significance. The largest possible thickness that preserves the integrity of the answers from (4.24) is determined by the number of discrete ordinates, the geometric thickness of the slab and the precision of the computing system.

It was shown that for $N = 2$, numerical stability requires that the largest optical thickness of the slab should be such that the largest eigenvalue $\lambda_1 < 709$ on a digital system operating with 16 significant digits arithmetic. For $N > 2$, and for a system operating with ν significant-digits arithmetic, it can be shown that $\lambda_1 < \gamma = (\nu+1)\ln 10$. The corresponding geometric thickness of the slab is $h < \gamma\mu_1/\sigma_t$ which we will call the γ-thickness criterion; μ_1 is the smallest positive directional cosine defined on the set of discrete ordinates $\{S_N\}$. For $\nu = 16$, we will have $\gamma \approx 40$ and $\lambda_1 < 40 \Rightarrow h < 40\mu_1/\sigma_t$. Clearly, a 40-thickness criterion is quite a severe limitation on the thickness of the slab. One way to avoid this problem is to stratify the slab into strata obeying the 40-thickness criterion.

Two contiguous strata are said to be similar if they have the same material composition, whether they have the same geometric thickness or not. In general two contiguous strata are not similar. Therefore, a heterogeneous slab is already stratified but if any one of its homogeneous strata is thicker than provided by the γ-thickness criterion, the stratum will have to be stratified into similar strata so that each stratum satisfies the criterion.

For a stratified slab of S strata, equation (4.24) may be written with indicial notation for the sth stratum as follows:

$$\left.\begin{aligned} \Psi^-_{m,s} &= \tau^n_{m,s}\Psi^-_{n,s+1} + \alpha^n_{m,s}\Psi^+_{n,s} + \rho^-_{m,s} \\ \Psi^+_{m,s+1} &= \alpha^n_{m,s}\Psi^-_{n,s+1} + \tau^n_{m,s}\Psi^+_{n,s} + \rho^+_{m,s+1} \end{aligned}\right\} \qquad m, n = 1, 2, \ldots, N'; s = 1, 2, \ldots, S \tag{6.1}$$

where s is the index for stratum; fluxes and radiances vectors are indexed by s at 0-boundary and $s + 1$ at h-boundary of the sth stratum. We readily recognize that (6.1) are the basis for an iteration algorithm to calculate fluxes at the boundaries of the slab, and eventually the flux distribution within the slab, be it homogeneous or heterogeneous. Numerical experimentations have shown that the most efficient iteration is the common sweeping algorithm of the diamond-difference method [8]. In any one iteration, the fluxes of the left side will be placed in the right side of the equations in the next iteration.

For the problem defined by (6.1) to be physically meaningful, it is imperative that all iterates $\Psi^{(k)}$ of the kth iteration are positive. In the case of $N = 2$, this condition is always satisfied for any positive initial guess of the fluxes. The proof is straightforward. Unfortunately, this proof cannot be extended to the general case of arbitrary N. For $L \geqslant 1$ and large N, some of the elements of matrix α could become negative. In that case it is impossible to rigorously prove that all iterates $\Psi^{(k)}$ are absolutely positive, nor is it possible to prove that any one iterate could become negative simply because one or a few elements of α are negative. We will assume that all iterates are positive. Our numerical experimentation could not prove otherwise. Similarly, the proof that the iteration based on (6.1) converges is not obvious. We have not encountered any convergence problem in our computations.

6.1. The method of Effective Albedo and Transmittance

The formal simplicity of (6.1) is somewhat misleading for it requires a large memory allocation and a large number of flops per iteration especially for heterogeneous and thick homogeneous slabs. An alternative approach to the iteration algorithm is possible. The new method amounts to calculating Effective Albedo and Transmittance (EAT) matrices of a slab from the matrices of the strata constituent of the slab. The method is valid for

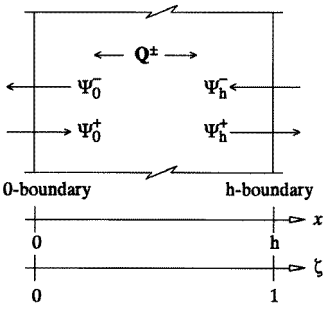

Figure 1. Nomenclature of boundary flux vectors for a slab of thickness h in x-representation and its normalized thickness in ζ-representation.

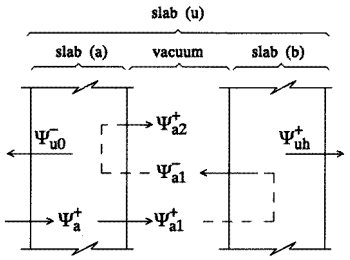

Figure 2. Nomenclature of flux vectors at the interfaces of a composite slab.

both homogeneous and heterogeneous slabs provided that any one individual stratum is homogeneous.

Consider two homogeneous sourceless slabs (a) and (b) characterized by α_a, τ_a, α_b and τ_b. The two slabs may be considered as two strata of one slab $(u) = (a) \cup (b)$ that can be a homogeneous or heterogeneous slab. Assume further that the two slabs are separated by vacuum space, 0-boundary of slab (a) is exposed to a boundary flux Ψ^+_{a0} and h-boundary of slab (b) is left unexposed (figure 2).

If slab (a) were alone, the exiting flux at its h-boundary would have been

$$\Psi^+_{a1} = \tau_a \Psi^+_{a0}. \tag{6.2}$$

In the presence of slab (b), this flux is going to be reflected by slab (b) as

$$\Psi^-_{a1} = \alpha_b \tau_a \Psi^+_{a0} \tag{6.3}$$

and flux Ψ^-_{a1} in turn is going to be reflected by slab (a) with the result that the exiting flux at h-boundary of (a) becomes

$$\Psi^{s+}_{a2} = \Psi^+_{a1} + \alpha_a \Psi^-_{a1}. \tag{6.4}$$

Rearrange (6.4) as follows:

$$\Psi^+_{a2} = (\boldsymbol{I} + \boldsymbol{A}_{ab})\tau_a \Psi^+_{a0} \tag{6.5}$$

where

$$\boldsymbol{A}_{ab} = \alpha_a \alpha_b. \tag{6.6}$$

The flux between the two slabs may be perceived as being 'trapped' in the cavity and it continues to bounce on the two slabs indefinitely with the result:

$$\Psi^+_{ah} = \left[\sum_{n=0}^{\infty} \boldsymbol{A}^n_{ab} \tau_a \right] \Psi^+_{a0}. \tag{6.7}$$

A necessary condition for the matrix power series in (6.7) to converge to a finite matrix is that the largest eigenvalue of matrix $\boldsymbol{A}_{ab}$ is less than 1. This can be proven directly using Sylvester's theorem [9] in association with Cauchy test of convergence [10]. However, the proof that this condition for convergence is always satisfied in the general case cannot be rigorously proven for matrix $\boldsymbol{A}_{ab}$. We will candidly assume that it is always satisfied in our problem, otherwise (6.7) will yield $\Psi^+_{ah} > \Psi^+_{a0}$, a violation to the principle of conservation of neutrons in a sourceless slab.

We recognize that the bracketed term of (6.7) is a transformation matrix that bears the significance of a transmittance operator of slab (a) relative to slab (b) for neutrons moving in the forward direction. Hence, we define a forward *effective transmittance* of slab (a) relative to slab (b) as

$$\tau_a^{eff+} = \theta_{ab}\tau_a \tag{6.8}$$

where

$$\theta_{ab} = \sum_{n=0}^{\infty} A_{ab}^n. \tag{6.9}$$

Clearly, matrix elements of τ_a^{eff+} must be such that $\|\tau_a^{eff+}\| > \|\tau_a\|$.

Further, the flux of (6.7) can be transmitted through slab (b) to obtain the exiting flux at h-boundary of slab (b). It can be reflected one more time with slab (b) then transmitted through slab (a) to obtain the exiting flux at 0-boundary of slab (a). This way the EAT properties of the composite slab (u) for the forward flux are obtained:

$$\tau_u^{eff+} = \tau_b\tau_a^{eff+} \tag{6.10}$$

$$\alpha_u^{eff+} = \alpha_a + \tau_a\alpha_b\tau_a^{eff+}. \tag{6.11}$$

Finally, the exiting fluxes at the extreme edges of (u) can be calculated directly using the EAT properties just calculated:

$$\Psi_{u0}^- = \alpha_u^{eff+}\Psi_{u0}^+ \tag{6.12}$$

$$\Psi_{uh}^+ = \tau_u^{eff+}\Psi_{u0}^+. \tag{6.13}$$

Continuing further, by recognizing that matrix product (6.6) is not commutative, in general, then α_u^{eff+} and τ_u^{eff+} are valid only for forward-flux boundary conditions. Another set of *backward* EAT properties of slab (u) that are valid for the backward flux can be obtained. Consequently, the general end-points solution for (2.1) in the sourceless slab (u) becomes

$$\Psi_{u0}^- = \tau_u^{eff-}\Psi_{uh}^- + \alpha_u^{eff+}\Psi_{u0}^+ \tag{6.14}$$

$$\Psi_{uh}^+ = \alpha_u^{eff-}\Psi_{uh}^- + \tau_u^{eff+}\Psi_{u0}^+. \tag{6.15}$$

Clearly, the forward and backward EAT matrices of slab (u) are not congruent except in the particular case where slabs (a) and (b) are identical.

Now we proceed to include radiance vectors in (6.14) and (6.15). Suppose, for the moment, that slab (a) contains a fixed distributed source. If the slab were alone surrounded by vacuum, then its radiance vectors ρ_{a0}^- and ρ_{ah}^+ are defined by (4.15) and (4.16). It can be shown that in the presence of slab (b) we will have

$$\rho_{ah}^{eff+} = \sum_{n=0}^{\infty} A_{ab}^n\rho_{ah}^+ = \theta_{ab}\rho_{ah}^+. \tag{6.16}$$

Expression (6.16) is formally identical to expression (6.7) except that flux vectors are exchanged with radiance vectors. It follows that the radiance vectors at the boundaries of slab (u) are obtained by the same transformations applied to flux vectors with the results:

$$\rho_u^{eff-} = \rho_{a0}^- + \tau_a\alpha_b\theta_{ab}\rho_{ah}^+ \tag{6.17}$$

$$\rho_u^{eff+} = \tau_b\theta_{ab}\rho_{ah}^+. \tag{6.18}$$

The *effective radiance vectors* (ERV) defined by (6.17) and (6.18) can now be inserted in the right-hand sides of (6.14) and (6.15), respectively. Other expressions for ERV can

be obtained for other prescribed source configurations by properly and orderly applying the same transformations.

In the foregoing, slabs (a) and (b) are separated by a vacuum space. The derivations continue to hold if the vacuum space is removed by bringing (a) and (b) into contact with each other. In that case, the flux of (6.7) becomes the forward flux at a point within slab (u), be it an arbitrary point within a homogeneous slab or the interface between two different media constituents of a heterogeneous slab. That way, one can calculate the forward and the backward fluxes at designated points within a slab to obtain the scalar flux and current as desired.

The EAT method just described for two strata can be applied to a slab containing any number of strata by merging one stratum at a time with previously merged strata. If the strata are piled up in the sequence $(a), (b), (c), \ldots, (z)$, say from left to right, the merger could be accomplished in the following sequence:

$$(u_1) = (a) \cup (b)$$
$$(u_2) = (u_1) \cup (c) \ldots \text{etc.}$$

At each step one should calculate the EAT and the ERV as appropriate. The number of mergers in this approach is equal to the number of strata less 1.

As regards the series θ_{rs}, they converge fairly quickly. The rate of convergence increases with the number of strata of a slab. This is because the strata become thin and the elements of their albedo matrices become quite small, enough to guarantee convergence to the desired precision with relatively small number of terms of the series. Also, since absorbers are poor reflectors, the convergence of series θ_{rs} should be quite fast in absorptive media.

An important feature of the EAT method is that it enables calculating exiting fluxes at the boundaries of the integrated slab without iterations thus saving a sizeable amount of memory allocations and CPU time. However, we recognize that the 40-thickness criterion could require large number of strata. This is particularly true if the slab is thick and a solution with large number of discrete ordinates is sought.

In the particular case of a thick homogeneous slab, the merger of the strata can be accelerated by merging (u_k)s with themselves, e.g.:

$$(u_1) = (a) \cup (b)$$
$$(u_2) = (u_1) \cup (u_1)$$
$$(u_3) = (u_2) \cup (u_2) \ldots \text{etc.} \tag{6.19}$$

That is, if the slab is made up of 2^n strata, only n mergers are needed to obtain the transformation matrices for one integral slab. Also, in this case, the EAT properties are invariant under rotation of a stratum about an axis at its midplane. Therefore, only one set of forward (or backward) properties is needed.

7. Numerical results

We consider the case of a homogeneous slab, 100 cm thick, stratified by the 40-thickness criterion in 2^n strata for various values of n. The thickness of each stratum and the number of strata for each n are shown in table 1. With this geometry, four neutronically different materials are used for test calculations. For that purpose, we selected the scattering moments shown in table 2 to demonstrate the performance of our numerical algorithms under extreme deep-penetration conditions. Indeed, the optical thickness that is determinable to numerical stabilities is the one defined along the direction given by the smallest directional cosine μ_1. In slab 4, this optical thickness is larger than 30 000 mfp; in slab 1 it is smaller than 10 mfp.

Table 1. Number of strata in a 100 cm slab. The thickness of a stratum is expressed in units of n and in centimetres.

n	No. of strata 2^n	Stratum thickness (cm)
0	1	100.000 000
2	4	25.000 000
3	8	12.500 000
4	16	6.250 000
5	32	3.125 000
6	64	1.562 500
7	124	0.781 250
8	256	0.390 625

Table 2. Macroscopic cross sections and scattering moments up to P_5 for four slabs used in the numerical calculations. All data are in cm^{-1}.

Slab	σ_t	σ_0	σ_1	σ_2	σ_3	σ_4	σ_5
1	1.00	0.99	0.80	0.40	0.20	0.10	0.05
2	3.00	1.00	0.80	0.40	0.20	0.10	0.05
3	1.00	0.99	−0.80	−0.40	−0.20	−0.10	−0.05
4	3.00	1.00	−0.80	−0.40	−0.20	−0.10	−0.05

Table 3. Scalar flux at the boundaries of slab 1 for different discrete ordinates N and different orders of anisotropic scattering. The thickness of the slab is measured in units of n, as in 2^n. All fluxes are in neutrons cm^{-2} s.

		P_1 scattering		P_3 scattering		P_5 scattering	
N	n	φ_0 $\times 10^1$	φ_h $\times 10^4$	φ_0 $\times 10^1$	φ_h $\times 10^4$	φ_0 $\times 10^1$	φ_h $\times 10^4$
	0	8.172 56	1.291 82				
2	4	8.172 56	1.291 82	—	—	—	—
	6	8.172 56	1.291 82				
	3	8.222 56	1.235 29	8.230 26	1.245 75		
4	6	8.222 56	1.235 29	8.230 26	1.245 75	—	—
	8	8.222 56	1.235 29	8.230 26	1.245 75		
	4	8.228 35	1.224 96	8.243 32	1.230 19	8.242 92	1.230 37
8	6	8.228 36	1.235 01	8.243 32	1.230 17	8.242 92	1.230 38
	8	8.228 36	1.235 01	8.243 32	1.230 17	8.242 92	1.230 38
	5	8.230 76	1.229 71	8.244 46	1.220 54	8.245 71	1.228 19
16	6	8.230 68	1.229 28	8.244 45	1.220 56	8.245 70	1.228 15
	8	8.230 84	1.220 30	8.244 27	1.229 33	8.245 72	1.228 28

The calculations were made with four sets of discrete ordinates $N = 2$, 4, 8 and 16. For each set of discrete ordinates the largest eigenvalue λ_1 was first obtained and the largest acceptable thickness of a stratum was determined, in centimetres and in n units.

The first set of flux calculations were done using the EAT method with entering flux boundary condition at 0-boundary: $\Psi_0^+ = \mathbf{1}$, and vacuum boundary condition at h-boundary.

Table 4. Scalar flux at the boundaries of slab 2 for different discrete ordinates N and different orders of anisotropic scattering. The thickness of the slab is measured in units of n, as in 2^n. All fluxes are in neutrons cm^{-2} s.

		P_1 scattering		P_3 scattering		P_5 scattering	
N	n	φ_0 $\times 10^1$	φ_h $\times 10^{120}$	φ_0 $\times 10^1$	φ_h $\times 10^{115}$	φ_0 $\times 10^1$	φ_h $\times 10^{115}$
	0	5.119 12	8.16(−39)*				
2	4	5.119 12	8.16(−39)	—	—	—	—
	6	5.119 12	8.16(−39)				
	5	5.181 83	0.005 82	5.167 72	0.002 98		
4	7	5.181 83	0.005 82	5.167 72	0.002 98	—	—
	8	5.181 83	0.005 82	5.167 72	0.002 98		
	6	5.197 11	2.707 23	5.188 31	2.791 68	5.187 69	4.483 61
8	7	5.197 11	2.707 23	5.188 31	2.791 68	5.187 69	4.483 61
	8	5.197 11	2.707 23	5.188 31	2.791 68	5.187 69	4.483 61
	5	—	—	—	—	—	—
16	6	5.200 65	2.749 17	5.198 94	3.495 98	5.191 51	4.281 69
	8	5.200 65	2.737 01	5.198 94	3.514 85	5.191 51	4.260 24

* read 8.16×10^{-39}.

Table 5. Scalar flux at the boundaries of slab 3 for different discrete ordinates N and different orders of anisotropic scattering. The thickness of the slab is measured in units of n, as in 2^n. All fluxes are in neutrons cm^{-2} s.

		P_1 scattering		P_3 scattering		P_5 scattering	
N	n	φ_0 $\times 10^1$	φ_h $\times 10^{11}$	φ_0 $\times 10^1$	φ_h $\times 10^{11}$	φ_0 $\times 10^1$	φ_h $\times 10^{11}$
	3	9.299 50	1.107 79	9.300 48	1.085 72		
4	6	9.299 50	1.107 69	9.300 49	1.085 70	—	—
	8	9.299 50	1.107 69	9.300 49	1.085 70		
	4	9.298 54	1.104 23	9.297 62	1.090 78	9.297 41	1.078 00
8	6	9.298 54	1.104 27	9.297 41	1.086 00	9.297 70	1.085 62
	8	9.298 54	1.104 27	9.297 41	1.086 00	9.297 70	1.085 62
	5	9.298 34	1.103 77	9.296 70	1.079 27	9.296 57	1.080 27
16	6	9.298 36	1.104 20	9.296 57	1.079 27	9.296 84	1.083 11
	8	9.298 36	1.104 31	9.296 56	1.079 37	9.296 83	1.082 70

The results of calculations are shown in tables 3, 4, 5 and 6 for all the slabs of table 2. We recognize that all fluxes are positive, despite that in many cases elements of the albedo matrix were negative. Indeed, we tested many other sets of cross sections. No negative fluxes were observed for as long as the thickness of any stratum is determined by the γ-criterion. All calculations were made on a PC-486 66 MHz using 16 significant digits arithmetic.

Another set of calculations were made using the iteration method formulated by (6.1).

Table 6. Scalar flux at the boundaries of slab 4 for different discrete ordinates N and different orders of anisotropic scattering. The thickness of the slab is measured in units of n, as in 2^n. All fluxes are in neutrons cm^{-2} s.

		P_1 scattering		P_3 scattering		P_5 scattering	
N	n	φ_0 $\times 10^1$	φ_h $\times 10^{134}$	φ_0 $\times 10^1$	φ_h $\times 10^{136}$	φ_0 $\times 10^1$	φ_h $\times 10^{137}$
	4	5.748 91	8.72(−21)*	5.762 21	7.44(−25)		
4	6	5.748 91	8.72(−21)	5.762 22	7.44(−25)	—	—
	8	5.748 91	8.72(−21)	5.762 22	7.44(−25)		
	5	5.728 67	4.38(−5)	5.754 42	1.02(−7)	5.804 50	1.11(−7)
8	6	5.736 95	4.56(−5)	5.746 88	1.68(−7)	5.747 95	7.89(−8)
	8	5.736 95	4.56(−5)	5.746 88	1.68(−7)	5.747 95	7.89(−8)
	6	5.725 48	7.24(+7)	—	—	—	—
16	7	5.733 94	2.452 31	5.743 00	5.588 07	5.743 81	6.989 07
	8	5.733 94	2.496 04	5.743 00	5.628 73	5.743 81	6.899 03

* Read 8.72×10^{-21}.

The convergence of the scalar flux was determined by the condition:

$$\left| \frac{\varphi^{(k)} - \varphi^{(k-1)}}{\varphi^{(k)}} \right| < 10^{-7}$$

where φ is the scalar flux and k the index of the current iteration. The same four slabs of table 2 were used. The results are identical to those obtained with the EAT method. Table 7 shows the fluxes at the boundaries of slab 1 and for the case of P_1 scattering; the other data are not reproduced in the interest of minimizing redundancy. The number of iterations needed to achieve convergence is quite large in this slab. In strongly absorbing slabs, the convergence is achieved within five iterations or less. In all calculations, we purposely avoided the implementation of any acceleration scheme to reveal the native characteristics of the method.

We compared our results of slab 1 in the case of linear anisotropy with those obtained with the SGF method [4]. They are identically the same up to $N = 8$ discrete ordinates; the SGF method works with linear anisotropy and cannot produce results for $N > 8$. By recognizing that the SGF calculations were compared with those obtained with the diamond-difference method [4], our method is, in effect, compared with the diamond-difference method. These comparisons show a net advantage in favour of the solution presented in this paper.

It is apparent from the results shown that the iteration method and the EAT method are equally good with respect to the precision of the flux. They produce identically the same flux except for a few anomalies illustrated in the flux at h-boundary shown in table 7 for $\{N, n\} = \{8, 8\}$. It takes an additional four iterations to converge to the same flux obtained with $n = 6$. This was accomplished by squeezing the convergence criterion to 10^{-8}.

Despite that the two methods produce the same flux, the preference is in favour of the EAT method. It is less demanding in memory allocation and it is faster than the iteration method. The iteration method begins to develop, as the EAT method does, after the transformation matrices are calculated for all strata. From that point further, more additional memory will have to be allocated and more computing time will be needed to perform the iteration than to calculate the EAT matrices.

Table 7. Scalar flux at the boundaries of slab 1 calculated using the iteration algorithm in P_1 scattering, for different discrete ordinates N. The thickness of the slab is measured in units of n, as in 2^n. All fluxes are in neutrons cm^{-2} s.

N	n	Iter.	φ_0 $\times 10^1$	φ_h $\times 10^4$
	0	1	8.172 56	1.291 82
2	4	23	8.172 56	1.291 82
	6	63	8.172 56	1.291 82
	3	29	8.222 56	1.235 29
4	6	64	8.222 56	1.235 29
	8	99	8.222 56	1.235 29
	4	37	8.228 35	1.224 96
8	6	60	8.228 36	1.225 01
	8	94	8.228 36	1.225 05
	5	47	8.230 76	1.229 71
16	6	58	8.230 68	1.229 27
	8	89	8.230 84	1.230 30

Another observation of merit is that, if the thickness of a stratum is the same, or slightly larger than the γ-thickness, the EAT method produces positive fluxes with the false impression that this is the solution to the problem at hand. We reproduced this situation in table 6 for $\{N, n\} = \{8, 5\}$ and $\{16, 6\}$. The fluxes are positive but they are the wrong solution; the iteration method diverges, or it gives negative fluxes in these cases. Therefore, the validity of the EAT method requires strict adherence to the γ-thickness criterion as no evidence of wrong answers will develop unless the thickness of the strata is substantially larger than the γ-thickness.

It was observed that, for $N > 4$, some of the elements of matrix α take negative values whether σ_l are positive or negative. In most cases an efficient remedy was to increase, or to decrease L by 2; the negative matrix elements then reverse to positive ones. In all cases, no negative flux was observed.

8. Summary

It is apparent from the foregoing that the closed-form solution to the discrete-ordinates transport equation can be expressed in pointwise form, or in end-points form without recourse to integral transforms. The distinct features of the proposed method are its ability to work with an arbitrary order of anisotropic scattering and the control of the round-off error.

Another feature of the proposed method is the one-sided boundary conditions. We converted the traditional one-dimensional neutron-transport problem, which is in effect a boundary-value problem, to another one functionally equivalent to an initial value problem in space. The domain of definition of this problem is, unlike the traditional initial value problem, closed by an upper bound equal to the spatial thickness of the slab. A constraint extracted from the solution itself and introduced as an auxiliary equation completed the closure of the solution.

One advantage of the proposed method is that it does not require a particular solution.

To the best of our knowledge, all non-integral transform methods previously discussed in the literature of discrete ordinates require *a priori* knowledge of a particular solution, the SGF method [4] is an illustration. Another advantage of the method is its excellent adaptability to numerical computations on a digital system. The round-off error is quite under control by the γ-thickness criterion.

The proposed method is devoted to the one-dimensional plane geometry problem in the one-speed approximation. The extension of the method to the multigroup problem is conceptually simple: develop a multigroup Λ matrix with group-to-group transfer submatrices $A_{g\to g'}$, and $A^*_{g\to g'}$, or solve the group equation and use the solution as a source term in the equations for the lower groups. In the former approach, Λ becomes a large sparse matrix. In the latter, the development of a recursive solution for systematic computations becomes imperative. We will examine this aspect of the problem in the future along with the extension of the method to the multidimensional geometry.

References

[1] Chandrasekhar S 1950 *Radiative Transfer* (Oxford: Oxford University Press)
[2] Davison B 1958 *Neutron Transport Theory* (Oxford: Oxford University Press)
[3] Larsen E W 1986 Spectral analysis of numerical methods for discrete ordinates problem *Trans. Theor. Stat. Phys.* **15** 93
[4] DeBarros R C and Larsen E W 1990 A numerical method for one-group slab-geometry discrete ordinates problems with no spatial truncation error *Nucl. Sci. Eng.* **104** 199
[5] DeBarros R C and Larsen E W 1992 A spectral nodal method for one-group x, y-geometry discrete ordinates problem *Nucl. Sci. Eng.* **111** 34
[6] Barichello L B and Vilhena M T 1993 A general analytic approach to the one-group, one-dimensional transport equation *Kerntechnik* **58** 3
[7] Vilhena M T and Barichello L B 1995 An analytical solution for the multigroup slab geometry discrete ordinates problems *Trans. Theor. Stat. Phys.* **24** 9
[8] Lewis E E and Miller Jr W F 1984 *Computational Methods of Neutron Transport* (New York: Wiley)
[9] Frazer R A, Duncan W J and Collar A R 1938 *Elementary Matrices* (Cambridge: Cambridge University Press)
[10] Oden J T 1979 *Applied Functional Analysis* (Englewood Cliffs, NJ: Prentice-Hall)